CHARGE-PARTICLE DYNAMICS IN AN ADIABATIC THERMAL BEAM EQUILIBRIUM

H. Wei and C. Chen, MIT, Combridge, MA 02139, U.S.A.

Abstract

Charged-particle motion is studied in the self-electric and self-magnetic fields of a well-matched, intense charged-particle beam and an applied periodic solenoidal magnetic focusing field. The beam is assumed to be in a state of adiabatic thermal equilibrium. The phase space is analyzed and compared with that of the well-known Kapchinskij-Vladimirskij (KV)-type beam equilibrium. It is found that the widths of nonlinear resonances in the adiabatic thermal beam equilibrium are narrower than those in the KV-type beam equilibrium. Numerical evidence is presented, indicating the absence of chaotic particle motion in the adiabatic thermal beam equilibrium.

INTRODUCTION

Several kinetic equilibria have been discovered for periodically focused intense charged-particle beams. Well-known equilibria for periodically focused intense beams include the Kapchinskij-Vladmirskij (KV) equilibrium in an alternating-gradient (AG) quadrupole magnetic focusing field [1,2] and the periodically focused rigid-rotor Vlasov equilibrium of the KV type in a periodic solenoidal magnetic focusing field [3,4]. Both of these beam equilibria [1-4] have a singular ($\delta-$function) distribution in the four-dimensional phase space. Such a $\delta-$function distribution gives a uniform density profile across the beam in the transverse directions, and a transverse temperature profile which peaks on axis and decreases quadratically to zero on the edge of the beam. Because of the singularity in the distribution functions, these beam equilibria are not likely to occur in real physical systems and cannot provide realistic models for theoretical and experimental studies and simulations except in the zero-temperature limit. For example, the KV equilibrium model cannot be used to explain the beam tails in the radial distributions observed in recent high-intensity beam experiments [5]. Recently, adiabatic thermal beam equilibria have been discovered in a periodic solenoidal magnetic focusing field [6-8] and an AG quadrupole magnetic focusing field [8,9]. The measured density distribution [5] matches that of the adiabatic thermal beam equilibrium in a spatially varying solenoidal magnetic focusing field [6,8].

There have been many studies of charged-particle dynamics in the KV-type equilibria [10-14]. These studies have shown that the phase space for the KV-type equilibria exhibits rich nonlinear resonances and chaotic seas for charged particles outside the beam envelope [10,11]. If charged particles cross the beam envelope due to perturbations, they may enter chaotic seas to form a beam halo or cause beam losses [12-14].

THEORY AND SIMULATION

We study charged-particle dynamics in the adiabatic thermal equilibrium of an intense charged-particle beam propagating with constant axial velocity $\beta_b c\hat{\mathbf{e}}_z$ in the periodic solenoidal magnetic focusing field

$$\mathbf{B}^{ext} = B_z(s)\hat{\mathbf{e}}_z - \frac{1}{2}\frac{dB_z(s)}{ds}\left(x\hat{\mathbf{e}}_x + y\hat{\mathbf{e}}_y\right), \qquad (1)$$

where $s=z$ is the axial coordinate, $B_z(s+S)=B_z(s)$ is the axial magnetic field, S is the fundamental periodicity length of the focusing field, and c is the speed of light in vacuum. The adiabatic thermal beam equilibrium has been derived under the paraxial approximation with the following assumptions: 1) $r_{brms} << S$, where r_{brms} is the RMS beam radius and 2) $\nu/\gamma_b^3\beta_b^2 << 1$, where $\nu = q^2 N_b/mc^2$ is the Budker parameter of the beam, q and m are the particle charge and rest mass, respectively, $N_b = \int_0^\infty n_b(r,s)2\pi r dr =$ const is the number of particles per unit axial length, and $\gamma_b = (1-\beta_b^2)^{-1/2}$ is the relativistic mass factor.

In the adiabatic thermal beam equilibrium [6-8], the beam density distribution is given by

$$n_b(r,s) = \frac{4\pi C\varepsilon_{th}^2}{r_{brms}^2(s)}\exp\left\{-\left[\frac{K}{2}+\frac{4\varepsilon_{th}^2}{r_{brms}^2(s)}\right]\frac{r^2}{4\varepsilon_{th}^2} - \frac{q}{\gamma_b^2 k_B T_\perp(s)}\phi(r,s)\right\}, \qquad (2)$$

and the self-electric potential $\phi(r,s)$ is determined by the Poisson equation

$$\frac{1}{r}\frac{\partial}{\partial r}\left(r\frac{\partial\phi}{\partial r}\right) = -4\pi q n_b(r,s) \qquad (3)$$

and the free-space boundary conditions. In Eqs. (2) and (3), C is a constant determined by $N_b = \int_0^\infty n_b(r,s)2\pi r dr$, $K \equiv 2q^2 N_b/\gamma_b^3 m\beta_b^2 c^2$ is the generalized beam perveance, $\varepsilon_{th} = \left[k_B T_\perp(s) r_{brms}^2/2\gamma_b m\beta_b{}^2 c^2\right]^{1/2}$ is the RMS thermal emittance in the Larmor frame, $\tilde{x} = x\cos\varphi - y\sin\varphi$ and $\tilde{y} = x\sin\varphi + y\cos\varphi$ where $\varphi = \int_0^s \sqrt{\kappa_z(s)}ds$, $T_\perp(s)$ is the Kelvin temperature of the beam, k_B is the Boltzmann

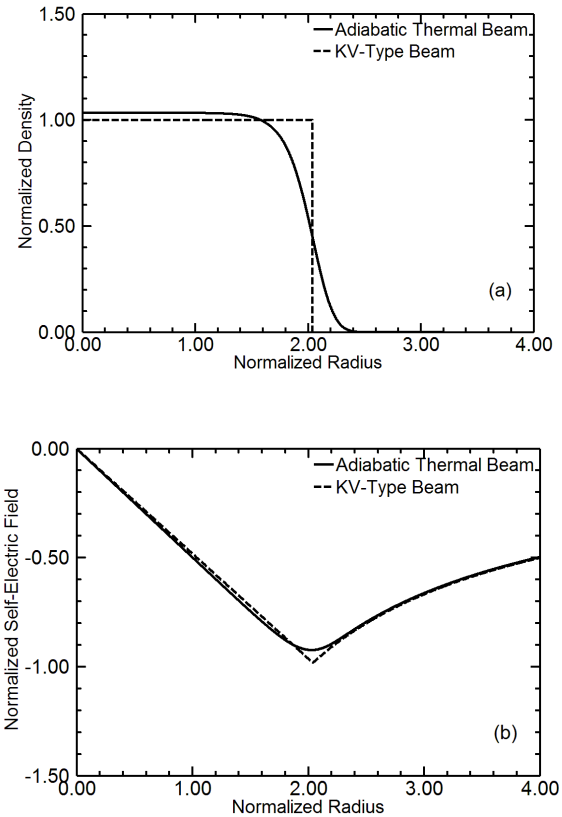

Figure 1: Plots of a) normalized density $n_b / n_{KV}(0,0)$ and b) normalized radial self-electric field $S^{3/2}KE_r / 4\varepsilon_{th}^{1/2} qN_b$ versus normalized radius $r/\sqrt{4\varepsilon_{th}S}$ in the KV-type beam equilibrium (dashed curve) and the adiabatic thermal beam equilibrium (solid curve) at $s=0$ for the same choice of system parameters as in Fig. 1. Here, $n_{KV}(0,0)$ is the density of the KV-type beam equilibrium at $s=0$ and $r=0$.

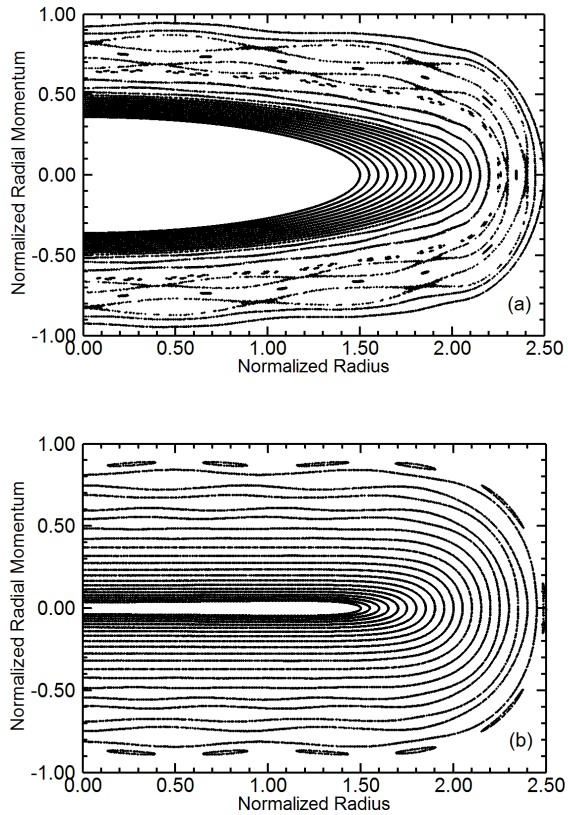

Figure 2: Poincare surface-of-section maps of charged-particle trajectories in a) KV-type beam equilibrium and b) adiabatic thermal beam equilibrium for $P_\theta = 0$ and the same choice of system parameters as in Fig. 1. Here, the normalized radial momentum is $(S/4\varepsilon_{th})^{1/2} dr/ds$ and the normalized radius is $r/\sqrt{4\varepsilon_{th}S}$.

constant, and the RMS beam envelope $r_{brms}(s) = r_{brms}(s+S)$ solves the beam envelope equation

$$\frac{d^2 r_{brms}}{ds^2} + \kappa_z(s) r_{brms} - \frac{K}{2r_{brms}} = \frac{4\varepsilon_{th}^2}{(1-\omega_b^2) r_{brms}^3} \qquad (4)$$

where $\sqrt{\kappa_z(s)} \equiv qB_z(s)/2\gamma_b m\beta_b c^2$ and $\omega_b^2 = 1 - (\varepsilon_{th}/\varepsilon_{\tilde{x}rms})^2$ with $\varepsilon_{\tilde{x}rms}$ being the RMS emittance in the $\tilde{x}$-direction.

Figure 1 shows a) density n_b and b) radial self-electric field E_r for the KV-type and adiabatic thermal beam equilibria at $s=0$ for the choice of system parameters corresponding to $S\sqrt{\kappa_z(s)} = (2/3)^{1/2}\sigma_0[1+\cos(2\pi s/S)]$, $SK/4\varepsilon_{th} = 7.0$, $\omega_b = 0$, and $\sigma_0 = 80°$. For $\omega_b = 0$, $\varepsilon_{th} = \varepsilon_{\tilde{x}rms}$ and the KV-type and adiabatic thermal beam equilibria have the same RMS beam envelopes. While the self-electric fields of the two beams are similar, there is an important difference: the electric field near the normalized radius $r/\sqrt{4\varepsilon_{th}S} \approx 2.0$ has a smooth transition from negative to positive slope for the adiabatic thermal beam equilibrium, whereas its radial derivative is discontinuous for the KV-type beam equilibrium.

The radial equation of motion of a charged particle in the cylindrical coordinates is

$$\frac{d^2 r}{ds^2} + \frac{P_\theta^2}{r^3} + \kappa_z(s) r + \frac{q}{\gamma_b^3 m\beta_b^2 c^2}\frac{\partial\phi(r,s)}{\partial r} = 0, \qquad (5)$$

where the canonical angular momentum P_θ is conserved.

Figure 2 shows a comparison between the Poincare surface-of-section maps of charged-particle trajectories in a) KV-type beam equilibrium and b) adiabatic thermal beam equilibrium for the choice of system parameters corresponding to $S\sqrt{\kappa_z(s)} = (2/3)^{1/2}\sigma_0[1+\cos(2\pi s/S)]$, $P_\theta = 0$, $\sigma_0 = 80°$, $\omega_b = 0$, and $SK/4\varepsilon_{th} = 7.0$. They are

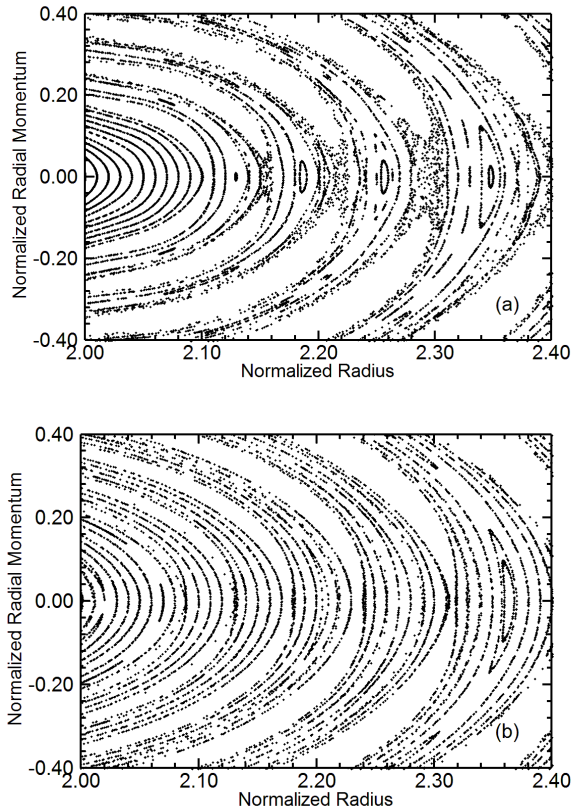

Figure 3: Close ups of Poincare surface-of-section maps of charged-particle trajectories for the two cases shown in Fig. 2.

generated by plotting (r, P_r) as a trajectory arrives at the lattice points $s/S = 0$, 1, 2…, 2000. For these parameters, the density for the KV-type beam equilibrium drops abruptly at $r/\sqrt{4\varepsilon_{th}S} \approx 2.0$, whereas the density for the adiabatic thermal beam equilibrium falls from its flat top value to almost zero between $r/\sqrt{4\varepsilon_{th}S} \cong 1.6$ and 2.4.

For $r/\sqrt{4\varepsilon_{th}S} < 2.0$, the phase space is regular in both the KV-type and adiabatic thermal beam equilibria, and the action of a charged particle in the KV-type beam is larger than that in the adiabatic thermal beam, as shown in Fig. 2. In the region $2 \le r/\sqrt{4\varepsilon_{th}S} \le 2.4$, however, there are striking differences between the KV-type and adiabatic thermal beam equilibria, as shown in Fig. 3. Comparing Fig. 4(a) with Fig. 4(b), there are two important differences to note. First, there are chaotic seas in the phase space of the KV-type beam, whereas chaotic motion is almost absent in the phase space of the adiabatic thermal beam equilibrium. Second, the widths of the nonlinear resonances in the adiabatic thermal beam equilibrium are narrower than those in the KV-type beam equilibrium.

CONCLUSION

We analyzed charged-particle motion in the self-electric and self-magnetic fields of a well-matched, intense charged-particle beam in a period solenoidal magnetic focusing field. We assumed that the beam is in the state of adiabatic thermal equilibrium. We compared the phase space of the adiabatic thermal beam equilibrium with that of a corresponding KV-type beam equilibrium. We found that the widths of some of the nonlinear resonances in the adiabatic thermal beam equilibrium are narrower than those in the KV-type beam equilibrium. We presented numerical evidence for the absence of chaotic particle motion in the adiabatic thermal beam equilibrium in a periodic solenoidal magnetic focusing field.

ACKNOWLEDGMENTS

The authors wish to thank Dr. Ksenia R. Samokhvalova and Dr. Jing Zhou for helpful discussions. This work was supported by US Department of Energy, Office of High Energy Physics, Grant No. DE-FG02-95ER40919, and Office of Fusion Energy Science, Grant No. DE-FG02-05ER54835. Research by H. Wei was also supported by the MIT Undergraduate Research Opportunity Program.

REFERENCES

[1] I.M. Kapchinskij and V.V. Vladimirskij, in Proc. Conf. High Energy Accel. (CERN, Geneva, 1959), p. 274.
[2] F. J. Sacherer, *Transverse Space-Charge Effects in Circular Accelerators* (Univ. of California, Berkley, Lawrence Radiation Laboratory, 1968).
[3] C. Chen, R. Pakter, and R. C. Davidson, Phys. Rev. Lett. **79**, 225 (1997).
[4] R. C. Davidson and H. Qin, *Physics of Intense Charged Particle Beams in High Energy Accelerators* (Imperial College Press, Singapore, 2001), p. 242.
[5] S. Bernal, B. Quinn, M. Reiser, abd P.G. O'Shea, Phys. Rev. ST Accel. Beams **5**, 064202 (2002).
[6] J. Zhou, K. R. Samokhvalova, and C. Chen, Phys. Plasmas **15**, 023102 (2008).
[7] K. R. Samokhvalova, J. Zhou, and C. Chen, Phys. Plasmas **14**, 103102 (2007).
[8] K. R. Samokhvalova, *Thermal Equilibrium Theory of Periodically Focused Charged-Particle Beams*, Ph.D Thesis, Massachusetts Institute of Technology, 2008.
[9] K. R. Samokhvalova, J. Zhou, and C. Chen, Phys. Plasmas **16**, 043115 (2009).
[10]L. M. Lagniel, Nucl. Instrum. Methods Phys. Res. **A345**, 1576 (1995).
[11] C. Chen, R. Pakter, and R.C. Davidson, Phys. Plasmas **6**, 3647 (1999).
[12] Q. Qian, R.C. Davidson, and C. Chen, Phys. Rev. **E51**, 5216 (1995).
[13] Y. Fink, C Chen, and W.P. Marable, Phys. Rev. **E55**, 7557 (1997).
[14] J. Zhou, B.-L. Qian, and C. Chen, Phys. Plasmas **11**, 4203 (2003).